Implications of the $D_s^+ \to \pi^+\pi^0\eta$ decay in the nature of $a_0(980)$ and molecular interpretation of the new $X_0(2900)$

Raquel Molina, Ju-Jun Xie, Wei-Hong Liang, Lisheng Geng and E. Oset

Table of contents

Introduction

Hadrons

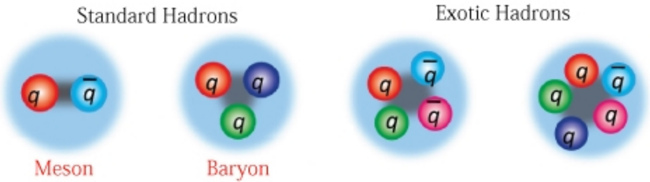

- 'Regular' hadrons: $q\bar{q}$, qqq

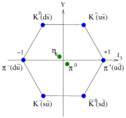

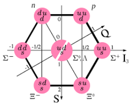

- Exotics: $q\bar{q}q\bar{q}$, $qqqq\bar{q}$, qqg,...

  Not $q\bar{q}$: $J^{PC} = 0^{+-}, 1^{-+}, 2^{+-}, 3^{-+}, \ldots$

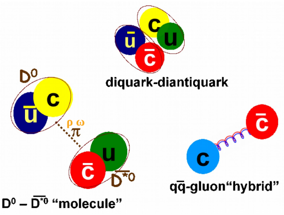

Dynamically Generated Resonances

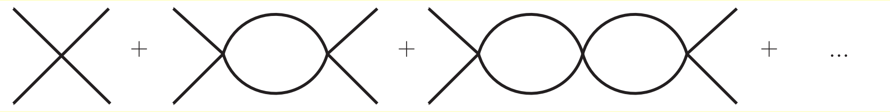

Examples

- σ, $a_0(980)$, $f_0(980)$... `Oller, Oset, Pelaez, PRL80(1998)`
- $N(1440)$ `Krehl, Hanhart, Krewald and Speth, PRC62(2000)`
- $\Lambda(1405)$ `Ramos, Oset, NPA635(1998); Jido, Meissner, Oller NPA725(2003); Hyodo, Weise PRC77(2008)`
- $P_c(4450)$ `Wu, Molina, Zou, Oset, PRL105(2010)`
- **New** **state** $X_0(2900)$ `Molina, Branz, Oset PRD82(2010)`

The $D_s^+ \to \pi^+\pi^0\eta$ decay and the nature of the $a_0(980)$

Is the $a_0(980)$ a threshold effect or a true resonance?

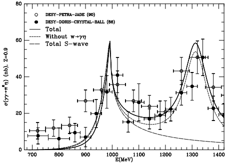

Figure 1: Integrated cross section for $\gamma\gamma \to \pi^0\eta$. Data: Oest(1990), Antreasyan(1986).

UChPT predictions

Channels: $K\bar{K}$, $\pi\eta$

Oller, Oset, NPA629(1998)

Guo, Liu, Oller, Rusetski, Meissner PRD95(2017)

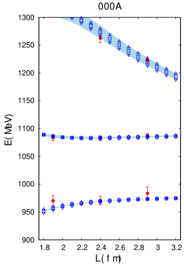

Figure 2: Fit to HadSpec data.

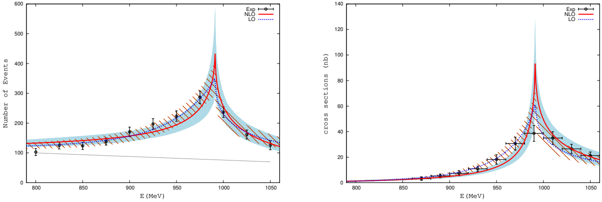

Figure 3: Left: $\pi\eta$ distribution. Data: WA76(1991). Right. Cross section $\gamma\gamma \to \pi\eta$. Data: Belle(2009).

Is the $a_0(980)$ a threshold effect or a true resonance?

Large N_c behaviour

“In particular, we have shown that the QCD large N_c scaling of the unitarized meson-meson amplitudes of chiral perturbation theory is in conflict with a $\bar{q}q$ nature for the lightest scalars [not so conclusively for the $a_0(980)$. The $a_0(980)$ behavior is more complicated. We cannot rule out a possible $\bar{q}q$ nature, or a sizable mixing], and strongly suggests a $\bar{q}\bar{q}qq$ or two-meson main component, maybe with some mixing with glue- balls, when possible.”

Pelaez, PRL92(2004)

Amplitude analysis of $\chi_{c1} \to \eta\pi^+\pi^-$

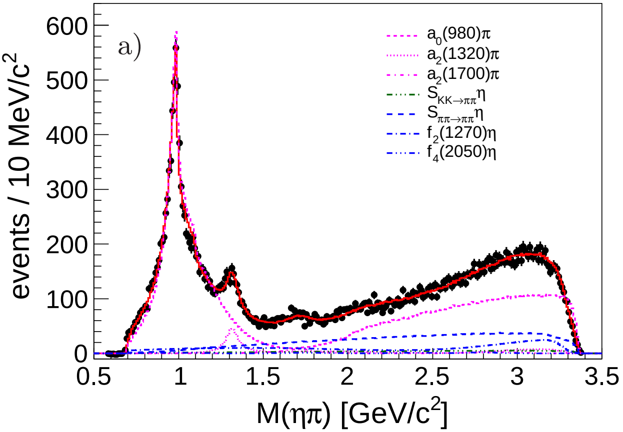

Figure 4: Projections in the (a)$\eta\pi$-invariant mass from data, compared with a base-line fit (solid curve) and corresponding amplitudes (various dashed and dotted lines) from PRD95(2017), BESIII.

BESIII: $D_s^+ \to \pi^+\pi^0\eta$

2019. BESIII has reported the so-called first observation of a pure W-annihilation decays $D_s^+ \to a_0^+(980)\pi^0$ and $D_s^+ \to a_0^0(980)\pi^+$

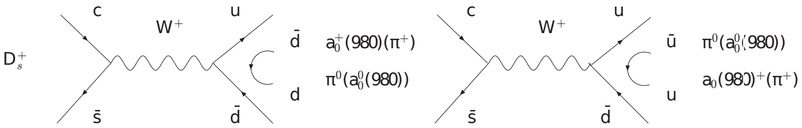

Figure 5: Annihilation mechanisms assumed in Ref.for the $D_s^+ \to \pi^0 a_0^+(980)$, $\pi^+ a_0^0(980)$. $\mathcal{B}[D_s^+ \to a_0(980)^+\pi^0,\ a_0(980)^+ \to \pi^+\eta] = (1.46 \pm 0.15 \pm 0.23)\%$

Topological classification of Weak decays

1. W-external emission
2. W-internal emission
3. W-exchange
4. W-annhilation
5. Horizontal W-loop
6. Vertical W-loop

L.L.Chau. PR(1983),PRD36(1987), PRD39(1989)

(Cabibbo favored) W-external emission? $D_s^+ \to \pi^+\bar{s}s$, but $\bar{s}s$ has $I = 0$. Requires $f_0(980)$ upon hadronization. Not good

$D_s^+ \to \pi^+\pi^0\eta$: W-internal emission PLB803(2020)

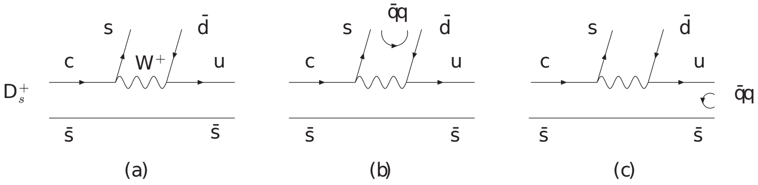

Figure 6: $D_s^+ \to \pi^0 a_0^+(980)$, $\pi^+ a_0^0(980)$: W internal emission mechanisms, (a) Primary step; (b) hadronization of the $s\bar{d}$ pair; (c) hadronization of the $u\bar{s}$ pair.

Hadronization

$$M = \begin{pmatrix} u\bar{u} & u\bar{d} & u\bar{s} \\ d\bar{u} & d\bar{d} & d\bar{s} \\ s\bar{u} & s\bar{d} & s\bar{s} \end{pmatrix},$$

$$\sum_i s\bar{q}_i q_i \bar{d} = \sum_i M_{3i} \qquad M_{i2} = (M^2)_{32},$$

$$\sum_i u\bar{q}_i q_i \bar{s} = \sum_i M_{1i} \qquad M_{i3} = (M^2)_{13},$$

$$(M^2)_{32} = \pi^+ K^- - \frac{1}{\sqrt{2}}\pi^0 \bar{K}^0,$$

$$(M^2)_{13} = \frac{1}{\sqrt{2}}\pi^0 K^+ + \pi^+ K^0,$$

$$H_1 = (\pi^+ K^- - \frac{1}{\sqrt{2}}\pi^0 \bar{K}^0) K^+,$$

$$H_2 = (\frac{1}{\sqrt{2}}\pi^0 K^+ + \pi^+ K^0) \bar{K}^0.$$

$D_s^+ \to \pi^0 a_0^+(980),\ \pi^+ a_0^0(980)$

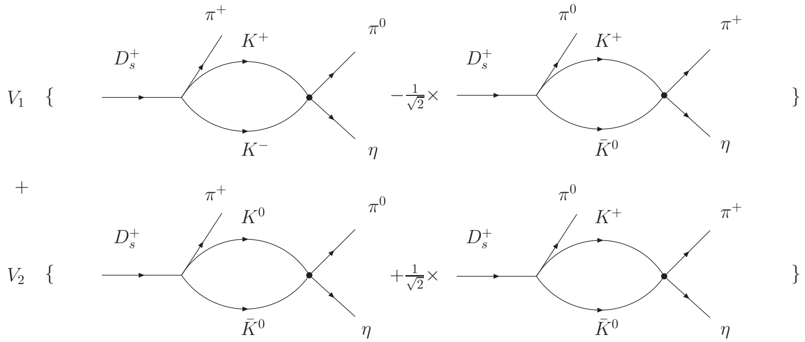

Figure 7: Diagrammatic representation of the $K\bar{K}$ final state interaction of the states H_1 and H_2 leading to $\pi^+\pi^0\eta$ in the final states.

$$
\begin{aligned}
t = \quad & V_1[G_{K\bar{K}}(M_{\pi^0\eta})t_{K^+K^-\to\pi^0\eta}(M_{\pi^0\eta}) - \frac{1}{\sqrt{2}}G_{K\bar{K}}(M_{\pi^+\eta})t_{K^+\bar{K}^0\to\pi^+\eta}(M_{\pi^+\eta})] \\
& + V_2[G_{K\bar{K}}(M_{\pi^0\eta})t_{K^0\bar{K}^0\to\pi^0\eta}(M_{\pi^0\eta}) + \frac{1}{\sqrt{2}}G_{K\bar{K}}(M_{\pi^+\eta})t_{K^+\bar{K}^0\to\pi^+\eta}(M_{\pi^+\eta})] \, ,
\end{aligned}
$$

$D_s^+ \to \pi^0 a_0^+(980),\ \pi^+ a_0^0(980)$

Chiral Unitary approach

$$\boxed{T = [1 - VG]^{-1} V}$$

Oller, Oset, Pelaez, PRL80(1998)

Xie, Dai, Oset, PLB742(2015)

$q_{\rm max} = 600$ MeV

Isospin

$$t_{K^+K^-\to\pi^0\eta} = -\frac{1}{\sqrt{2}} t^{I=1}_{K\bar{K}\to\pi\eta},$$

$$t_{K^0\bar{K}^0\to\pi^0\eta} = \frac{1}{\sqrt{2}} t^{I=1}_{K\bar{K}\to\pi\eta},$$

$$t_{K^+\bar{K}^0\to\pi^+\eta} = -t^{I=1}_{K\bar{K}\to\pi\eta},$$

We obtain,

$$\boxed{t = \bar{V}\left[G_{K\bar{K}}(M_{\pi^0\eta}) t^{I=1}_{K\bar{K}\to\pi\eta}(M_{\pi^0\eta}) - G_{K\bar{K}}(M_{\pi^+\eta}) t^{I=1}_{K\bar{K}\to\pi\eta}(M_{\pi^+\eta})\right]}$$

with $\bar{V} = (V_2 - V_1)/\sqrt{2}$.

Note that, with the isospin multiplets (u, d), $(-\bar{d}, \bar{u})$,

$$|s\bar{d} >= -|1/2, 1/2 > \qquad |s\bar{d}, u\bar{s} >= -|1, 1 >$$

$$|u\bar{s} >= |1/2, 1/2 > \qquad |\pi a_0; I = 1, I_3 = 1 >= \frac{1}{\sqrt{2}}|\pi^0 a_0^+ - \pi^+ a_0^0 >$$

$D_s^+ \to \pi^0 a_0^+(980),\ \pi^+ a_0^0(980)$

Invariant mass distribution

$$\frac{d^2\Gamma}{dM_{\pi^0\eta}dM_{\pi^+\eta}} = \frac{1}{(2\pi)^3}\frac{M_{\pi^0\eta}M_{\pi^+\eta}}{8M_{D_s^+}^2}|t|^2$$

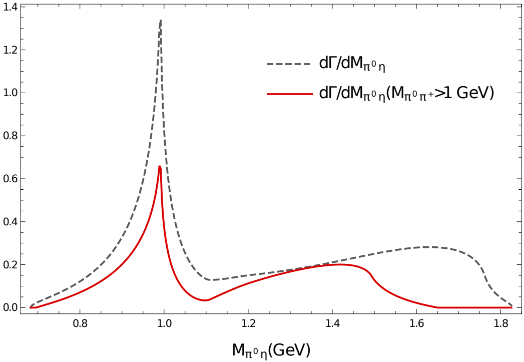

Figure 8: $d\Gamma/dM_{\pi^0\eta}$ as a function of $M_{\pi^0\eta}$. Dashed line with no $M_{\pi^+\pi^0}$ restriction. Solid line with the restriction of $M_{\pi^+\pi^0} > 1$ GeV.

$D_s^+ \to \pi^0 a_0^+(980)$, $\pi^+ a_0^0(980)$

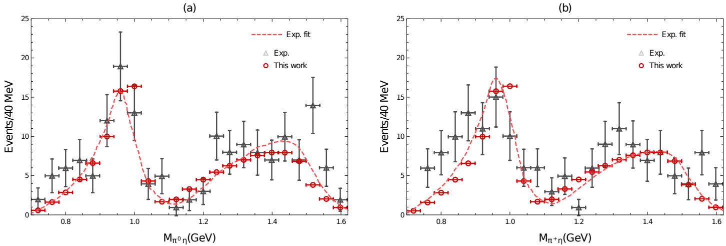

Figure 9: Event distribution in 40 MeV bins of $d\Gamma/dM_{\pi\eta}$ compared with experiment with $M_{\pi^+\pi^0} > 1$ GeV. (a) for $\pi^0\eta$ distribution; (b) for $\pi^+\eta$ distribution. The dashed lines are taken from [1] after the non πa_0 events are removed. Molina, Xie, Liang, Geng and Oset, PLB803(2020)

[1] BESIII Collaboration, PRL123(2019)

But...this is not the end of the story!

$D_s^+ \to \pi^0 a_0^+(980)$, $\pi^+ a_0^0(980)$

Arxiv: 2102.0534, Ling, Liu, Lu, Geng and Xie

Inspired in the work of Hsiao et al., EPJC80(895), the authors find that both mechanisms, internal and external-W emission through triangle diagrams are relevant.

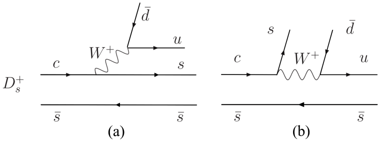

Figure 10: a) External W-emission mechanism for $D_s^+ \to \rho^+\eta$ and b) internal W-conversion mechanisms.

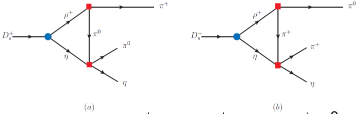

Figure 11: $D_s^+ \to (\rho^+\eta \to)\pi^+\pi^0\eta$.

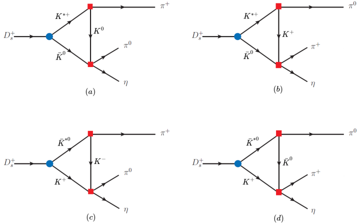

Figure 12: Triangle rescattering diagrams for $D_s^+ \to (K^{*0}\bar{K}^0 \to)\pi^+\pi^0\eta$ and $D_s^+ \to (K^+\bar{K}^{*0} \to)\pi^+\pi^0\eta$.

The new state $X_0(2900)$

New flavor exotic tetraquark ($C = -1; S = 1$)

LHCb (2020)

Two states $J^P = 0^+, 1^-$ decaying to $\bar{D}K$. First clear example of an heavy-flavor exotic tetraquark, $\sim \bar{c}\bar{s}ud$.

$$X_0(2866) : M = 2866 \pm 7 \quad \text{and} \quad \Gamma = 57.2 \pm 12.9\,\text{MeV},$$
$$X_1(2900) : M = 2904 \pm 5 \quad \text{and} \quad \Gamma = 110.3 \pm 11.5\,\text{MeV}.$$

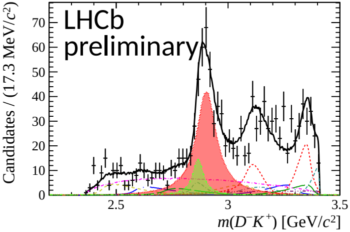

D. Johnson (CERN), LHC seminar, $B \to DDh^-$; a new (virtual) laboratory for exotic searches at LHCb p. August 11 (2020)

Vector-vector scattering Bando,Kugo,Yamawaki

$$\mathcal{L}_{III} = -\frac{1}{4}\langle V_{\mu\nu} V^{\mu\nu}\rangle$$

$$\mathcal{L}_{III}^{(3V)} = ig\langle(\partial_\mu V_\nu - \partial_\nu V_\mu) V^\mu V^\nu\rangle$$

$$\mathcal{L}_{III}^{(c)} = \frac{g^2}{2}\langle V_\mu V_\nu V^\mu V^\nu - V_\nu V_\mu V^\mu V^\nu\rangle$$

$V_{\mu\nu}$ =

$$\partial_\mu V_\nu - \partial_\nu V_\mu - ig[V_\mu, V_\nu]$$

$$g = \frac{M_V}{2f}$$

V_μ =

$$\begin{pmatrix} \frac{\rho^0}{\sqrt{2}} + \frac{\omega}{\sqrt{2}} & \rho^+ & K^{*+} & \bar{D}^{*0} \\ \rho^- & -\frac{\rho^0}{\sqrt{2}} + \frac{\omega}{\sqrt{2}} & K^{*0} & D^{*-} \\ K^{*-} & \bar{K}^{*0} & \phi & D_s^{*-} \\ D^{*0} & D^{*+} & D_s^{*+} & J/\psi \end{pmatrix}_\mu$$

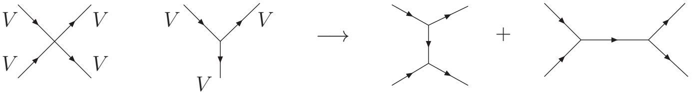

a) b) c) d)

New flavor exotic tetraquark ($C = 1, S = -1$)

Molina,Branz,Oset, PRD82(2010)

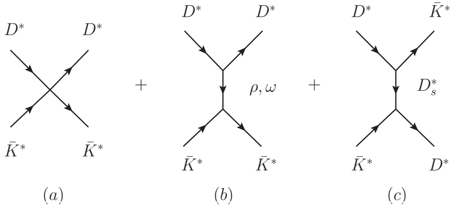

Figure 13: The $D^*\bar{K}^* \to D^*\bar{K}^*$ interaction at the tree level; (a) contact term; (b) exchange of light vectors; (c) exchange of a heavy vector.

J	Amplitude	Contact	V-exchange	$\sim$ Total
0	$D^*\bar{K}^* \to D^*\bar{K}^*$	$4g^2$	$-\frac{g^2(p_1+p_4).(p_2+p_3)}{m^2_{D^*_s}} + \frac{1}{2}g^2(\frac{1}{m^2_\omega} - \frac{3}{m^2_\rho})(p_1+p_3).(p_2+p_4)$	$-9.9g^2$
1	$D^*\bar{K}^* \to D^*\bar{K}^*$	0	$\frac{g^2(p_1+p_4).(p_2+p_3)}{m^2_{D^*_s}} + \frac{1}{2}g^2(\frac{1}{m^2_\omega} - \frac{3}{m^2_\rho})(p_1+p_3).(p_2+p_4)$	$-10.2g^2$
2	$D^*\bar{K}^* \to D^*\bar{K}^*$	$-2g^2$	$-\frac{g^2(p_1+p_4).(p_2+p_3)}{m^2_{D^*_s}} + \frac{1}{2}g^2(\frac{1}{m^2_\omega} - \frac{3}{m^2_\rho})(p_1+p_3).(p_2+p_4)$	$-15.9g^2$

Table 1: Tree level amplitudes for $D^*\bar{K}^*$ in $I = 0$. Last column: $(V_{\rm th.})$.

New flavor exotic tetraquark ($C = 1, S = -1$)

Spin projectors

$$T = [\hat{1} - VG]^{-1} V$$

$$\mathcal{P}^{(0)} = \frac{1}{3}\epsilon_\mu \epsilon^\mu \epsilon_\nu \epsilon^\nu$$

$$\mathcal{P}^{(1)} = \frac{1}{2}(\epsilon_\mu \epsilon_\nu \epsilon^\mu \epsilon^\nu - \epsilon_\mu \epsilon_\nu \epsilon^\nu \epsilon^\mu)$$

$$\mathcal{P}^{(2)} = \{\frac{1}{2}(\epsilon_\mu \epsilon_\nu \epsilon^\mu \epsilon^\nu + \epsilon_\mu \epsilon_\nu \epsilon^\nu \epsilon^\mu) - \frac{1}{3}\epsilon_\mu \epsilon^\mu \epsilon_\nu \epsilon^\nu\} .$$

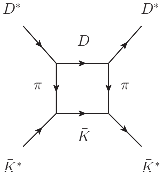

$I(J^P)$	M[MeV]	Γ[MeV]	Channels	state
$0(2^+)$	2572	23	$D^*K^*, D_s^*\phi, D_s^*\omega$	$D_{s2}(2572)$
$0(1^+)$	2707	-	$D^*K^*, D_s^*\phi, D_s^*\omega$	?
$0(0^+)$	2683	71	$D^*K^*, D_s^*\phi, D_s^*\omega$	?

Table 2: States with $C = 1, S = 1, I = 0$.

$I(J^P)$	M[MeV]	Γ[MeV]	Channels	state
$0(2^+)$	2733	36	$D^*\bar{K}^*$	?
$0(1^+)$	2839	-	$D^*\bar{K}^*$	?
$0(0^+)$	2848	59	$D^*\bar{K}^*$	$X_0(2866)$

Table 3: States with $C = 1, S = -1, I = 0$.

New flavor exotic tetraquark ($C = 1, S = -1$)

Two-meson loop function:

$$G_i(s) = \frac{1}{16\pi^2}\Bigg(\alpha + \mathrm{Log}\frac{M_1^2}{\mu^2} + \frac{M_2^2 - M_1^2 + s}{2s}\mathrm{Log}\frac{M_2^2}{M_1^2} + \frac{p}{\sqrt{s}}\Big(\mathrm{Log}\frac{s - M_2^2 + M_1^2 + 2p\sqrt{s}}{-s + M_2^2 - M_1^2 + 2p\sqrt{s}} + \mathrm{Log}\frac{s + M_2^2 - M_1^2 + 2p\sqrt{s}}{-s - M_2^2 + M_1^2 + 2p\sqrt{s}}\Big)\Bigg),$$

Form factor (box-diagram):

$$F(q) = e^{((p_1^0 - q^0)^2 - \vec{q}^{\,2})/\Lambda^2} \qquad \text{Navarra, PRD65(2002)} \tag{1}$$

with $q_0 = (s + m_D^2 - m_K^2)/2\sqrt{s}$, $\Lambda \sim 1 - 1.3$ GeV. Previous work (2010): $\alpha = -1.6$ (with $\mu = 1500$ MeV) and $\Lambda = 1200$. Recent work: Molina, Oset PLB811 2020, $\alpha = -1.474$, $\Lambda = 1300$.

$$\mathcal{L} = \frac{iG'}{\sqrt{2}}\epsilon^{\mu\nu\alpha\beta}\langle\delta_\mu V_\nu \delta_\alpha V_\beta P\rangle$$

$$\mathcal{L}_{VPP} = -ig\langle[P, \partial_\mu P]V^\mu\rangle$$

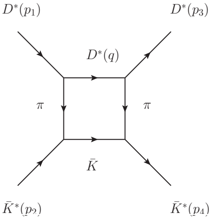

Decay of the $D^*\bar{K}^*$ states to $D^*\bar{K}$

$$-it = \frac{9}{2}(G' g m_{D^*})^2 \int \frac{d^4q}{(2\pi)^4} \epsilon^{ijk}\epsilon^{i'j'k'} \left(\frac{1}{(p_1-q)^2 - m_\pi^2 + i\epsilon}\right)^2$$
$$\times \frac{1}{q^2 - m_{D^*}^2 + i\epsilon} \frac{1}{(p_1+p_2-q)^2 - m_K^2 + i\epsilon}$$
$$\times \epsilon^{j(1)}\epsilon^{m(2)}\epsilon^{k(3')} q^i q^m \epsilon^{j'(1)}\epsilon^{m'(4)}\epsilon^{k'(3')} q^{i'} q^{m'} F^4(q) \qquad (2)$$

Taking now into account that,

$$\int \frac{d^3q}{(2\pi)^3} f(\vec{q}^{\,2}) q^i q^m q^{i'} q^{m'} = \frac{1}{15} \int \frac{d^3q}{(2\pi)^3} f(\vec{q}^{\,2}) \vec{q}^{\,4} (\delta_{im}\delta_{i'm'} + \delta_{ii'}\delta_{mm'} + \delta_{im'}\delta_{m'i}) \ ,$$

one obtains,

$$4\epsilon^{j(1)}\epsilon^{m(2)}\epsilon^{j(3)}\epsilon^{m(4)} - \epsilon^{j(1)}\epsilon^{j(2)}\epsilon^{m(3)}\epsilon^{m(4)} - \epsilon^{j(1)}\epsilon^{m(2)}\epsilon^{m(3)}\epsilon^{j(4)} \ ,$$

which is a combination of the spin projectors, $5\mathcal{P}^{(1)} + 3\mathcal{P}^{(2)}$, zero component for $J = 0$ (violates parity). Taking q on-shell,

$$\boxed{\mathrm{Im}\, t = -\frac{3}{2}\frac{1}{8\pi}(G' g m_{D^*})^2 q^5 \left(\frac{1}{(m_D^* - \omega^*(q))^2 - \omega^2(q)}\right)^2 \frac{1}{\sqrt{s}} F^4(q)}$$

Decay of the $D^*\bar{K}^*$ states to $D^*\bar{K}$

$I(J^P)$	$M[\mathrm{MeV}]$	$\Gamma[\mathrm{MeV}]$	Coupled channels	state
$0(2^+)$	2775	38	$D^*\bar{K}^*$	?
$0(1^+)$	2861	20	$D^*\bar{K}^*$	?
$0(0^+)$	2866	57	$D^*\bar{K}^*$	$X_0(2866)$

Table 4: New results including the width of the D^*K channel.

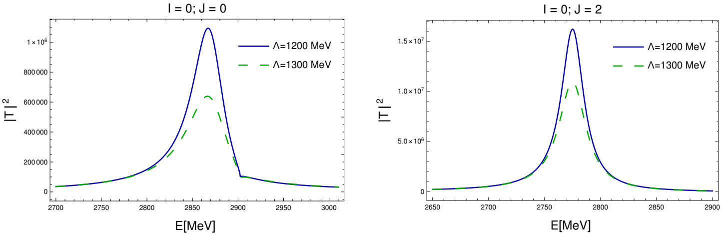

Figure 14: $|T|^2$ for $C = 1, S = -1, I = 0, J = 0$ and $J = 2$.

Decay of the $0(1^+)$ state to $D^*\bar{K}$

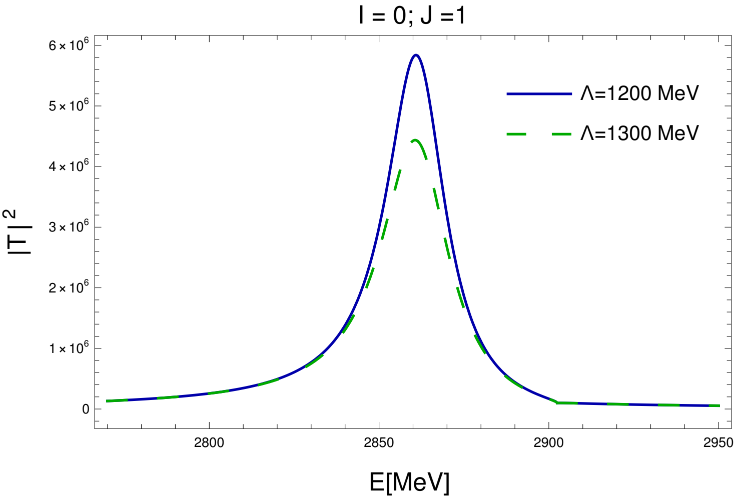

Figure 15: $|T|^2$ for $C = 1, S = -1, I = 0, J = 0$ and $J = 1$.

Conclusions

Conclusions

- The $D_s^+ \to \pi^+\pi^-\eta$ through the $a_0(980)$ proceeds via W-internal/external emission and not W-annhilation.
- The new BESIII data and the analysis shown here supports the $a_0(980)$ as a dynamically generated resonance from the $\pi\eta$ and $K\bar{K}$ channels.
- The new discovered $X_0(2900)$ is compatible with a $\bar{D}^*K^*(D^*\bar{K}^*)$ molecular state and there should be other similar states with $J^P = 1^+, 2^+$.